Applied Surface Science 280 (2013) 124–131

Contents lists available at SciVerse ScienceDirect

Applied Surface Science

journal homepage: www.elsevier.com/locate/apsusc

Comparison of corrosion properties of passive films formed on phase reversion induced nano/ultrafine-grained 321 stainless steel☆

Lv Jinlong, Luo Hongyun*

Key Laboratory of Aerospace Materials and Performance (Ministry of Education), School of Materials Science and Engineering, Beijing University of Aeronautics and Astronautics, Xueyuan Road 37, Beijing 100191, China

ARTICLE INFO

Article history:
Received 30 November 2012
Received in revised form 15 April 2013
Accepted 17 April 2013
Available online 30 April 2013

Keywords:
Nano/ultrafine
Mott–Schottky plots
Corrosion resistance
Stainless steels

ABSTRACT

The nano/ultrafine grain (NUG) with an average grain size of 230 nm was obtained by cold rolling down to 94% reduction in thickness and reversion annealing at 800 °C for 200 s. The NUG sample exhibited a lower corrosion resistance than coarse grain (CG) sample in 0.1 M NaCl solution at room temperature, indicating that the passive film formed on the surface of the NUG austenite did not improve corrosion resistance in the solution. However, the corrosion resistance of the former was higher than that of the latter in 0.5 M H_2SO_4 solution at room temperature, which was proved by electrochemical impedance spectroscopy and Mott–Schottky plots in conjunction with the point defect model. Comparing slightly difference of acceptor density (i.e. cation vacancies) between CG and NUG samples, higher corrosion resistance of NUG sample was probably attributed to significant decreased donor density (i.e. oxygen vacancies and cation interstitials) in 0.5 M H_2SO_4 solution. Moreover, the corrosion resistance of the passive films formed on CG and NUG samples in borate buffer solution at room temperature showed little difference.

1. Introduction

It is known that many austenitic stainless steels are unstable at room temperature so that austenite can be transformed to martensite by deformation [1]. In subsequent annealing, the martensite can be reverted to austenite and lead to noticeable grain refinement. The special nano/ultrafine grain was obtained by controlling phase reversion annealing temperature and amount of cold rolling [1–3], leading to an excellent tensile strength–ductility combination [1,4] and fatigue behavior [5]. Moreover, High-cycle fatigue behavior of ultrafine-grained (UFG) 17Cr–7Ni Type 301LN austenitic stainless and high-Mn Fe–22Mn–0.6C TWIP steels were investigated [6]. As far as we know, very few researchers elaborated corrosion behavior of nano/ultrafine grain by the same fabrication processing [7]. Hamada et al. [7] reported the submicron-grained structure of AISI 301LN austenitic stainless steel exhibited better pitting corrosion resistance than the coarse-grained one in the acidic chloride solution and also in immersion in the ferric chloride solution. In contrast, contradictory results about the effect of grain refinement on corrosion resistance were reported. Wang and Li [8] reported that nanocrystallisation obtained by sandblasting and annealing process improved the stability of the passive film on 304 stainless steels surface, which resulted from the increase of electron work function. Balusamy et al. [9] showed that nanocrystallisation and high defect density induced by a surface mechanical attrition treatment increased the corrosion resistance of 409 stainless steels. However, Zheng et al. [10] reported that thickness and composition of the passive film formed in 0.5 M H_2SO_4 at room temperature on both as-received and nanocrystalline 304 stainless steel by equal channel angular pressed (ECAP) showed little difference. The improved corrosion resistance of ECAPed stainless steels was not caused by thickness or composition change, but by compactness and stability improving of the passive films. The nanocrystalline surface on 316L stainless steels fabricated by cavitation–annealing led to a lower susceptibility to pitting corrosion and higher repassivation power in 0.9 wt.% NaCl solution at 25 °C [11]. While Ye et al. [12] found that nanocrystalline 309 stainless steels by DC magnetron sputtering exhibited different corrosion resistance in different solutions.

The improved corrosion resistance of nanocrystallised materials by surface nanocrystallisation processes [12] was commonly interpreted using the theory of much more diffusion paths (grain boundaries) in nanocrystalline material for chromium to enrich in the passive film [13]. However, the correlative studies showed the improved corrosion resistance of nanocrystalline due to more chromium diffusion was not significant at room temperature [10]. It was shown that the comprehension of passivity and its protective character against corrosion were closely connected with the electronic properties of passive films [14]. The anodic passive film

* Corresponding author. Tel.: +86 10 82339905; fax: +86 10 82317128.
E-mail addresses: ljlhit@126.com (L. Jinlong), luo7128@163.com (L. Hongyun).

0169-4332/$ – see front matter © 2013 The Authors. Published by Elsevier B.V. All rights reserved.
http://dx.doi.org/10.1016/j.apsusc.2013.04.108

as suggested by Chao et al. [15] contained a high concentration of point defect such as metal vacancies, electrons and holes. It was shown that the passive film on most metals exhibited a semiconducting behavior [15]. However, the semiconductor type was affected by component of the passive film and corrosion environment. The results of the capacitance response indicated that the passive films on low carbon steel behaved like highly doped n-type semiconductors in borate buffer solution, which showed that the passive film properties were dominated by iron [16]. The passive film on Ni exhibited a p-type semiconducting property irrespective of the solution temperature in pH 8.5 buffer solution [17]. The passive film on Cr behaved as an n-type semiconductor in 0.5 M H_2SO_4 [18]. However, the Mott–Schottky plots slop indicated a p-type semiconductivity of the passive films formed on chromium in 0.5 M H_2SO_4 [19]. Moreover, in NaF and NaCl aqueous solutions, Cl^- and F^- ions competed in affecting the semiconducting type of passive films formed on microcrystalline Al [20].

Above results suggested that complex mechanism of the passive film formation and grain refinement obtained by the reversion transformation processing could affect thickness and composition of the passive film on stainless steel. These could affect corrosion resistance of stainless steel. Therefore, the objective of this work was to evaluate the effect of the NUG obtained by heavily cold rolled and phase reversion annealing on semiconductor characteristics and corrosion resistance of passive films on stainless steel. Mechanisms responsible for corrosion resistance in different solutions were discussed.

2. Experimental procedure

2.1. Sample preparation

The material used in this paper is a 321 stainless steel plate with a chemical compositions (wt.%) as follows: 0.05C, 1.44Mn, 0.6Si, 17.8Cr, 9.1Ni, 0.035P, 0.002S, 0.21Ti and balance Fe. The as-received samples were annealed for 30 min at 1050 °C. The 2 mm sheet was cold rolled to 94% total thickness reduction by 15 stages with uniform thickness reduction in a laboratory rolling mill at room temperature and was subsequently annealed for reversion transformation at 800 °C for 200 s. Following annealing, the samples were water quenched. The volume fraction of strain-induced was measured by Dimension Icon X-ray diffraction (XRD) with a diffractometer using Cu Kα. Before XRD, all the samples after the reversion transformation processing were electro-polished to remove any possible deformation-induced martensite on the surface due to sample preparation. The electropolishing was carried out at a voltage of 20 V at −25 °C. The electrolyte solute was 5 ml $HClO_4$ + 95 ml ethanol. A JEM-2100F transmission electron microscopy (TEM) was used to examine the microstructure.

2.2. Electrochemical tests

The samples were sealed in holders with acid resistant epoxy resin in order to expose to the electrolyte a planar area of 1 cm^2. Pretreatment was consisted of mechanical polishing on a fine grade emery paper followed by polishing using a soft cloth with alumina as grinding paste, degreasing in acetone, rinsing with distilled water and drying in air at room temperature. The electrochemical cell employed in this study was made of glass beaker with the three electrodes. Very high density graphite and a saturated calomel electrode (SCE) were used as the counter and the reference electrodes, respectively. The electrochemical measurements were performed using the electrochemical workstation 660 B model (CHI company) controlled by a PC. The double loop electrochemical potentiokinetic reactivation (DLEPR) test was conducted in 0.5 M H_2SO_4 + 0.01 M KSCN solution [21]. The experiment was started after nearly steady state open circuit potential (OCP) had been reached (about 30 min). The potential swept in the anodic direction at 1 mV s^{-1} until the potential of 0.3 V_{SCE} was reached, then the scan was reversed until the open circuit potential. The role of KSCN was to help to break the passive film during the reactivation cycle of the test.

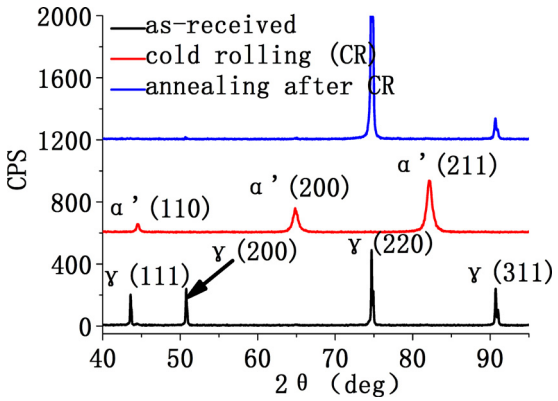

Fig. 1. The XRD patterns for as-received, 94% cold rolling and 94% cold rolled and reversion annealing.

The potentiodynamic polarization curves were obtained in 0.1 M NaCl solution, 0.5 M H_2SO_4 solution and borate buffer solution (0.075 M $Na_2B_4O_7{\cdot}10H_2O$ + 0.05 M H_3BO_3), respectively. The scan rates of the potentiodynamic polarization curves were 10 mV s^{-1} and 0.5 mV s^{-1}, respectively. The open circuit potential, the electrochemical impedance spectroscopy (EIS) and Mott–Schottky measurements were carried out in 0.5 M H_2SO_4 solution and borate buffer solution after samples were immersed for 60 min. The capacitance measurements were carried out on samples at a fixed frequency of 1000 Hz using an excitation voltage of 5 mV. The potential sweeping rate was 50 mV s^{-1} considering the assumption of "frozen-in defect structure" for the Mott–Schottky theory. The EIS measurements were performed at the open circuit potential after samples were immersed for 60 min using a frequency range of 100 kHz to 10 mHz and a 5 mV amplitude of the AC signal at room temperature.

3. Results and discussion

3.1. Microstructure characterization

The phase change investigated by X-ray diffraction in the thermomechanical process is shown in Fig. 1. The as-received sample is austenite and its microstructure is shown in Fig. 2a. After the cold rolling, the sample was changed completely to a′-martensite phase in Fig. 1. The TEM micrograph in Fig. 2b shows martensite with a high density of dislocations. The dislocation slip is the main mechanism of grain refinement by the dislocation cell and dislocation substructure. The grain is refined remarkably, which is consistent with broadening of diffraction peak in the result of X-ray diffraction. After annealing at 800 °C for 200 s, martensite is transformed to austenite again in Fig. 1. The microstructure is consisted of nearly equiaxed γ-grains with an average grain size of 230 nm in Fig. 2c. It is worthwhile to note that the CG austenite phase does not have a preferred orientation, while nano/ultrafine austenite phase expands along a preferred orientation the (2 2 0)γ plane in Fig. 1, while the most densely packed crystallographic plane (1 1 1)γ is almost disappeared. The texture significantly affected the corrosion behavior. Sample with the most densely packed crystallographic plane parallel to the surface was found to offer the highest corrosion resistance, regardless of their grain size. Considering the low stacking fault energy of austenitic stainless steels, annealing twins